

Structure and orientation of small molecules dissolved in the liquid crystalline phases of CsPFO/water system by multinuclear NMR†

Silvia Borsacchi, Donata Catalano* and Carlo Alberto Veracini

Received 29th January 2009, Accepted 26th March 2009

First published as an Advance Article on the web 22nd April 2009

DOI: 10.1039/b901895f

Pyridine, L-alanine and L-phenylalanine dissolved in the liquid crystalline phases of the lyotropic system CsPFO/water are studied by means of ^2H , ^{13}C and ^1H NMR. The orientational order parameters of the solutes are determined in a wide temperature range, together with some relevant geometrical parameters. In particular, a prevailing conformation for L-phenylalanine interacting with the micelle is suggested and, for all solutes, convincing representations of their specific interactions with the micelle surface are inferred. From ^{19}F and ^{13}C NMR spectra in the nematic phase, the orientational order parameters for the perfluorooctanoate chain inside the micelles are estimated.

Introduction

NMR spectroscopy in liquid crystalline phases (LX-NMR) has been extensively and successfully used for the last forty years to investigate the orientational order and the molecular structure of mesogenic molecules and solutes partially oriented in mesophases.^{1,2}

These pieces of information are obtainable from the anisotropic parts of the spin interactions which dominate the NMR spectra in liquid crystalline phases, namely dipolar and quadrupolar couplings. LX-NMR has been mainly applied to the study of thermotropic liquid crystals and, consequently, the most studied molecules dissolved in liquid crystalline solvents are hydrophobic compounds.

The possibility of obtaining structural information from partially averaged dipolar couplings has also been introduced in the complex practice of protein structural analysis,³ where such “residual” dipolar couplings have been successfully used for refining structures obtained by conventional NMR approaches or X-ray crystallography.⁴

Looking at relatively small molecules oriented in lyotropic mesophases, dipolar couplings of oligosaccharides and oligopeptides (see for instance ref. 5 and 6) have been measured and analyzed. In these cases, information on molecular orientation, conformations and flexibility is obtained from rather extended sets of dipolar couplings, whose absolute values do not exceed 10 Hz and whose relative signs cannot be easily inferred. Therefore, the experimental data set is not directly analyzed, but it is compared to those obtained by quantummechanical computational methods for single or fast exchanging conformers, with different orientational assumptions. This procedure has also been applied to systems closely related to those studied in this paper, that is to alanine dipeptide⁷ and tetraalanine in the liquid crystalline phases of the binary

mixture Cs-perfluorooctanoate/water (CsPFO/ H_2O).⁶ Here we present a LX-NMR study performed on small molecules in the same solvent, applying the traditional LX-NMR approach, well consolidated in thermotropic solvents, that is extracting the strictly entangled structural and orientational information directly from experimental quadrupolar and dipolar couplings. In the binary mixture CsPFO/ H_2O (or CsPFO/ D_2O),^{8,9} beyond the critical micellar concentration, the surfactant molecules aggregate in disk-shaped micelles, forming an isotropic and two liquid crystalline phases, the nematic (N_D^+) and the lamellar (L_D) one, respectively. The director of such phases (defined by the average direction of the axis perpendicular to the disk's surface) aligns parallel to the magnetic field, as expected considering the high positive diamagnetic anisotropy of the fluorinated alkyl chains. This system has been extensively studied because of its many peculiarities.^{8,10–12} The most relevant ones, for this study, are the stability of the nematic phase over a wide range of concentrations and temperatures, compared with other common lyotropic systems, and the fact that even the so called lamellar phase is formed by finite, relatively small easily orientable disk-shaped aggregates. As far as the use of the CsPFO/water mixture as lyotropic solvent is concerned, the wholly fluorinated core of the micelles is certainly repellent to non-fluorinated chemical compounds, in particular to hydrophilic solutes.¹³ Thus, in these mesophases, hydrophilic molecules are essentially dissolved in water, only interacting with the charged surface of the micelles and with the counter-ions layer.

The first part of this work concerns the study of the order of the PFO chains through the analysis of ^{19}F and ^{13}C spectra in the nematic phase of the CsPFO/ D_2O mixture. The solutes chosen for this work were pyridine, alanine and phenylalanine; along such sequence the complexity of the tackled problem increases. Pyridine (perdeuterated, in the present work), a rigid molecule well studied by LX-NMR in thermotropic systems,^{14–16} was here investigated by means of ^2H -NMR. Alanine, for which a detailed structural theoretical study is available,¹⁷ is a small amino acid whose orientational behaviour could be

Dipartimento di Chimica e Chimica Industriale, Università di Pisa, via Risorgimento 35, 56126, Pisa, Italy. E-mail: donata@cci.unipi.it

† Electronic supplementary information (ESI) available: Fig. S1–S3; Table S1. See DOI: 10.1039/b901895f

studied by a set of ^1H – ^1H , ^{13}C – ^1H and ^{15}N – ^1H dipolar couplings. Phenylalanine is a more complex, flexible system, for which we combined the analysis of ^2H quadrupolar couplings and ^1H – ^1H dipolar couplings. In all cases the spectral data analysis essentially consisted of the fitting of the anisotropic experimental couplings to their analytical expressions using the Saupe formalism, suitable for rigid molecules in uniaxial mesophases.^{2,18} Of course, at least phenylalanine could not be considered rigid *a priori*, but, as will be shown, the indication of a prevailing “effective” conformation came out of this study.

It is worth noticing that, in lyotropic aqueous media, the solute–solvent interactions are different from—and more complicated than—those in thermotropic mesophases: they involve interacting ions and take place mainly at the complex interfaces between amphiphilic aggregates and water. As a serious consequence for data analysis, the average orientation of the solute with respect to the phase director cannot be easily presumed. Nevertheless, convincing representations of the specific interactions between the three solute molecules and the micelle surface could be obtained.

Summary of theory^{1,2}

The relevant experimental quantities in LX-NMR are the ZZ components (Z is the direction of the magnetic field) of the anisotropic parts of the σ , J , D , q tensors, describing the chemical shielding, scalar, dipolar and quadrupolar nuclear interaction, respectively, averaged on fast intramolecular and reorientational motions. These quantities will be indicated, for a couple of nuclei ij , as $\tilde{A}_{ijZZ}^{\text{aniso}}$'s. For a rigid molecule (or molecular fragment), in an uniaxial phase with the director uniformly aligned along the magnetic field, $\tilde{A}_{ijZZ}^{\text{aniso}}$ is related to the order parameters of the molecule as follows:

$$\tilde{A}_{ijZZ}^{\text{aniso}} = \frac{2}{3} \sum_{\alpha,\beta} S_{\alpha\beta} A_{\alpha\beta}^{ij} \quad (1)$$

$A_{\alpha\beta}^{ij}$ are the components of the A_{ij} interaction tensor in the molecular axes frame (α, β, γ) and $S_{\alpha\beta}$ are the order parameters, elements of the symmetric, traceless Saupe matrix:

$$S_{\alpha\beta} = \left\langle \frac{3 \cos \theta_{Z\alpha} \cos \theta_{Z\beta} - \delta_{\alpha\beta}}{2} \right\rangle \quad (2)$$

where $\theta_{Z\alpha}$ is the angle between the α molecular axis and the Z axis, while the brackets indicate time averaging on fast reorientational motions.

The $S_{\alpha\beta}$ values (a maximum of 5 independent numbers ranging from -0.5 to 1) can be obtained from a set of experimental $\tilde{A}_{ijZZ}^{\text{aniso}}$'s, provided that an adequate number of $A_{\alpha\beta}^{ij}$ components is known.

By applying to the Saupe matrix the usual rules for the rotation of matrices, the order parameter S_{xx} of the generic x direction, fixed on the molecule, can be expressed as:

$$S_{xx} = \sum_{\alpha,\beta} \cos \theta_{x\alpha} S_{\alpha\beta} \cos \theta_{\beta x} \quad (3)$$

where $\theta_{x\alpha}$ is the angle between the x and α directions.

A molecule dissolved in the aqueous bulk of a lyotropic LX phase and interacting with the partially ordered micelles,

experiences at least two different sites where isotropic and anisotropic reorientation, respectively, occur. In the quite usual condition of fast exchange, the experimental value $\tilde{A}_{ijZZ}^{\text{aniso}}$ is the weighted average of the values at each site. This turns into the fact that each experimental order parameter $S_{\alpha\beta}$ corresponds to that of the interacting molecules subset, scaled by their fraction.

In this work we will exploit the quadrupolar interaction of deuterium nuclei and the dipolar couplings between several nuclei (^1H , ^2H , ^{13}C , ^{15}N , ^{19}F).

The experimental quadrupolar splitting of the signal of a deuteron i , $\Delta\nu_q^i$ can be expressed as:

$$\Delta\nu_q^i = \left| \frac{3}{2} q_{aa}^i \left[S_{aa}^i + \frac{\eta^i}{3} (S_{bb}^i - S_{cc}^i) \right] \right| \quad (4)$$

where S_{aa}^i , S_{bb}^i and S_{cc}^i are the order parameters of the principal axes (a, b, c) of q^i , the electric field gradient tensor on the nucleus, q_{aa}^i , q_{bb}^i , q_{cc}^i are its principal elements in order of decreasing value, and $\eta^i = \frac{q_{bb}^i - q_{cc}^i}{q_{aa}^i}$ is its asymmetry parameter. The a axis can be generally considered collinear to the C–Dⁱ bond. For sp^3 C atoms, η^i presumably vanishes, while, for aromatic carbons, c is perpendicular to the ring plane and η^i assumes a small positive value. Moreover, safely transferable values of q_{aa} and η typical of deuterons bond to sp , or sp^2 or sp^3 hybridized C atoms are reported in the literature. Finally, if the S_{aa}^i , S_{bb}^i and S_{cc}^i order parameters are expanded using eqn (3), $\Delta\nu_q^i$ is obtained as a linear combination of the molecular order parameters relative to the (α, β, γ) frame, so recovering an expression of the form of eqn (1).

The dipolar coupling between nuclei i and j is usually defined as $D_{ij} = 1/2 \tilde{D}_{ijZZ}^{\text{aniso}}$. D_{ij} is related to nuclear, structural and order parameters by the following equation:

$$D_{ij} = -\frac{K_{ij}}{r_{ij}^3} S_{ij} \quad (5)$$

Here $K_{ij} = \frac{\gamma_i \gamma_j}{4\pi^2} h$ (γ_i is the gyromagnetic ratio of the i nucleus), r_{ij} is the internuclear distance and S_{ij} is the order parameter of the ij direction, which is also often expressed, using eqn (3), as a linear combination of the molecular order parameters. In eqn (5) corrective terms due to harmonic and anharmonic vibrations have been neglected. Eqn (3) and (5) can be usefully combined to express D_{ij} as a linear combination of the molecular order parameters relative to the (α, β, γ) frame (see eqn (1)).

^1H -NMR and ^{13}C -NMR spectra in liquid crystalline phases are dominated by homonuclear and heteronuclear dipolar couplings, respectively, which split each isotropic signal into a multiplet. The scalar couplings J_{ij} also contribute to the experimental splittings $\Delta\nu_{ij}$, but, for both ^1H – ^1H and ^{13}C – ^1H interactions, the anisotropic part $\tilde{J}_{ijZZ}^{\text{aniso}}$ can usually be neglected with respect to $\tilde{D}_{ijZZ}^{\text{aniso}}$. In the case of two magnetically equivalent nuclei i, j , the experimental dipolar splitting is:

$$\Delta\nu_{\text{dip}}^i = 3|D_{ij}| \quad (6a)$$

For magnetically non-equivalent nuclei and in the limit of first-order spectra, as certainly occurs for heteronuclear coupling ($\gamma_i \neq \gamma_j$), one has

$$\Delta\nu_{\text{dip}}^i = |2D_{ij} + J_{ij}^{\text{iso}}| \quad (6b)$$

The J_{ij}^{iso} values must be determined from isotropic spectra and subtracted from the experimental splittings to obtain the D_{ij} values.

In summary, for determining the order parameters of the molecule (or of a molecular rigid fragment), the experimental quadrupolar and dipolar couplings can be fitted to eqn (4) and (5), respectively. Both expressions, after the suitable substitutions performed using eqn (3), become linear combinations of the molecular order parameters, whose coefficients depend on the molecular geometry. In this work, the geometry will be mainly assumed from the literature and corrected only in some details to better match the experimental data. Actually, in the case of the flexible phenylalanine, two conformational angles will also be determined by data fitting.

Experimental

Materials and samples

CsPFO was prepared as described in ref. 8. Pentadecafluorooctanoic acid (96%) and CsOH were obtained from Aldrich. The pH value of the various solutions was checked by means of Pehanon indicator paper strips (Macherey Nagel) with gradation 0.2, at room temperature.

Two samples of lyotropic solution were prepared: the first contained CsPFO and D₂O, with weight fraction $w_{\text{CsPFO}}/w_{(\text{CsPFO} + \text{D}_2\text{O})} = 0.39$; the second one contained H₂O instead of D₂O, with higher weight fraction ($w_{\text{CsPFO}}/w_{(\text{CsPFO} + \text{H}_2\text{O})} = 0.46$). The measured pH value was 7.5 ± 0.1 for both samples.

Pyridine-d₅ was obtained from Aldrich; it was dissolved in CsPFO/D₂O, with concentration $w_{(\text{pyridine-d}_5)}/w_{\text{D}_2\text{O}} \sim 5 \times 10^{-2}$. The measured pH of this sample was 8.8 ± 0.1 .

L-Alanine-¹⁵N (98%) was obtained from Cambridge Isotope Laboratories Inc., unlabeled L-alanine (purity >99%) was purchased from Fluka; the labeled and unlabeled amino acids were dissolved in two amounts of CsPFO/D₂O, respectively. For both samples the final concentration was $w_{(\text{L-alanine})}/w_{\text{water}} \sim 10^{-3}$, the measured pH value was 7.8 ± 0.1 .

L-Phenylalanine-d₈ (98%) was obtained from Cambridge Isotope Laboratories Inc. and dissolved in CsPFO/H₂O. The sample concentration was $w_{(\text{L-phenylalanine-d}_8)}/w_{\text{H}_2\text{O}} \sim 10^{-3}$, the measured pH value was 7.8 ± 0.1 . A similar sample was prepared dissolving unlabeled L-phenylalanine (Aldrich) into the CsPFO/D₂O mixture.

NMR Spectra and phase transition temperatures

All NMR spectra were recorded with a Varian VXR300 spectrometer operating at 299.95 MHz, 270 MHz, 75.43 MHz and 46.04 MHz on ¹H, ¹⁹F, ¹³C and ²H, respectively. The temperature of the samples was controlled within ± 0.1 °C. The 90° pulse width was 26 μs for ¹H and ¹⁹F, 12 μs for ¹³C and 10 μs for ²H.

CsPFO/D₂O and CsPFO/H₂O systems. ²H NMR, ¹⁹F and ¹³C single pulse spectra were recorded on the CsPFO/D₂O sample with suitable numbers of scans, in the range of temperature between 35 °C and 20 °C, that is from the isotropic (I) into the nematic (N_D⁺) and lamellar (L_D) phases, with intervals of 0.5 °C or 1 °C between measurements. An

analogous series of ²H NMR spectra was recorded on the CsPFO/H₂O system, with as many scans as required to detect the natural abundance D₂O signal. The transition temperatures of the CsPFO/D₂O mixtures were $T_{(\text{I} \rightarrow \text{N}_\text{D}^+) } = 32.5 \text{ °C} \pm 0.5 \text{ °C}$ and $T_{(\text{N}_\text{D}^+ \rightarrow \text{L}_\text{D}) } = 26.5 \text{ °C} \pm 0.5 \text{ °C}$, those of the CsPFO/H₂O mixture were three degrees higher, respectively, according to published phase diagrams.^{8,9}

Pyridine-d₅ in CsPFO/D₂O. ²H-NMR spectra were recorded between 30.0 °C and 20.1 °C, in steps of 0.3 °C, with 32 scans each and an acquisition time of 1.6 s. The spectra revealed that the high solute concentration had considerably lowered the isotropic–nematic transition temperature: the oriented phase appeared only below 24.9 °C.

L-Alanine in CsPFO/D₂O and L-alanine-¹⁵N in CsPFO/D₂O. ¹H-NMR spectra were recorded, on both samples, with 64 scans and an acquisition time of 2 s, between 34 °C and 22 °C, in steps of 1 °C. Two phase transitions were observed: from isotropic to nematic ($T_{(\text{I} \rightarrow \text{N}_\text{D}^+) } = 29.5 \text{ °C} \pm 0.5 \text{ °C}$) and from nematic to lamellar phase ($T_{(\text{N}_\text{D}^+ \rightarrow \text{L}_\text{D}) } = 25.5 \text{ °C} \pm 0.5 \text{ °C}$) in both cases. ¹³C-NMR spectra were recorded, with and without ¹H decoupling, at 32 °C, 28 °C and 24 °C, that is in the isotropic, nematic and lamellar phases, respectively, on both samples.

L-Phenylalanine-d₈ in CsPFO/H₂O. ²H-NMR spectra were recorded with 512 scans and an acquisition time of 1 s between 35 °C and 23 °C, in steps of 1 °C. The observed transition temperatures were: $T_{(\text{I} \rightarrow \text{N}_\text{D}^+) } = 33.0 \text{ °C} \pm 0.5 \text{ °C}$ and $T_{(\text{N}_\text{D}^+ \rightarrow \text{L}_\text{D}) } = 28.0 \text{ °C} \pm 0.5 \text{ °C}$. A further spectrum was recorded with 20 000 scans at 25 °C.

L-phenylalanine in CsPFO/D₂O. ¹H-NMR spectra were recorded between 33 °C and 23 °C, in steps of 2 °C, with 4000 scans and an acquisition time of 1 s. The transition temperatures were about 1 °C lower than those of the previous sample.

Results and discussion

CsPFO/D₂O system

In the series of ²H NMR spectra recorded on the CsPFO/D₂O sample between 35 °C and 20 °C, the sudden passage from a single peak to a quadrupolar doublet marks the transition from the isotropic to the nematic phase. The quadrupolar splitting regularly increases with decreasing temperature, until an evident change of the slope marks the nematic to lamellar phase transition (see Fig. 1).

In the isotropic ¹⁹F NMR spectrum seven structured signals are present, unambiguously assigned in the literature.¹⁹ When the nematic phase is entered, the extended network of ¹⁹F–¹⁹F dipolar splittings broadens the spectrum and makes it completely unresolved, except for the CF₃ signal, which, at least at 31–32 °C, appears as an isolated, hardly resolved triplet (Fig. S1 in ESI†). Such a structure is due to the dipolar interaction inside the system of three equivalent nuclei (the possible $\tilde{J}_{\text{FFZZ}}^{\text{aniso}}$ contribution²⁰ can be neglected in this rough analysis). Since the ¹⁹F–¹⁹F splitting between nearby components of the triplets, $\Delta \nu_{\text{dip}}^{\text{FF}}$, is about 1440 Hz at 32 °C,

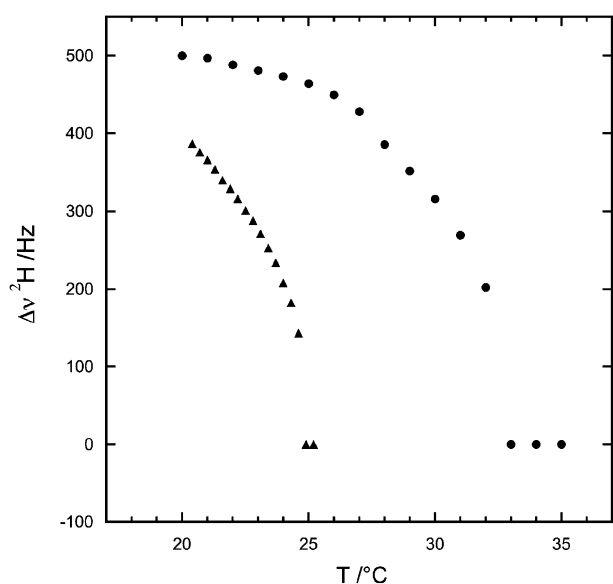


Fig. 1 Trend with temperature of deuterium quadrupolar splitting of D₂O in CsPFO/D₂O (●) and CsPFO/D₂O containing pyridine-d₅ (▲).

through eqn (6a) and (5), knowing that $K_{FF} = 106264.9 \text{ Å}^3 \text{ s}^{-1}$ and assuming $r_{FF} = 2.21 \text{ Å}$, we obtain $S_{FF} \sim -0.05$. The choice of negative sign for S_{FF} (positive sign for $\Delta\nu_{\text{dip}}^{\text{FF}}$) is based on the presumption that the F–F direction inside the CF₃ group, inside the micelle, is mainly perpendicular to the micelle axis and, therefore, to the magnetic field. If a condition of local effective cylindrical symmetry around the C–CF₃ axis occurs, S_{ij} (the order parameter of whichever ij direction forming an angle θ with the C–CF₃ axis) is related to S_{CC} as follows:²

$$S_{ij} = \frac{3 \cos^2 \theta - 1}{2} S_{CC} \quad (7)$$

Assuming tetrahedral geometry of the CF₃ group and applying eqn (7) twice, we estimate $S_{CC} \sim 0.10$ and $S_{CF}^{CF_3} \sim -0.03$ at 32 °C.

The assignments of the ¹⁹F-decoupled ¹³C NMR spectra in the isotropic and lamellar phases of the CsPFO/D₂O sample are reported in ref. 21 and 22, respectively. In all the recorded ¹³C NMR spectra the signal relative to the carboxylic ¹³C nucleus is isolated at high frequencies, while all the others are closely grouped. At the isotropic–nematic transition, wide dipolar triplets appear, one for each ¹³C bonded to two ¹⁹F nuclei, while the terminal CF₃ group originates a narrow quartet, as clearly shown in ref. 22 by means of a 2D SLF spectrum. In our single-pulse spectra all such multiplets superimpose, producing a rough and broad but well recognizable triplet (under which the CF₃ quartet is hidden) throughout the nematic phase (Fig. S2 in ESI†). The splittings related to different CF₂ groups must therefore be all similar and the resulting effective splitting ranging from 2800 to 5600 Hz, representative of the “average” ¹³C–¹⁹F interaction along the PFO chain, the ends excepted, can be analyzed through eqn (6b) and (5). Assuming $J_{CF}^{\text{iso}} \sim -270 \text{ Hz}$ and $r_{CF} = 1.36 \text{ Å}$,²² and knowing that $K_{CF} = 28400.6 \text{ Å}^3 \text{ s}^{-1}$, we obtain an $S_{CF}^{CF_2}$ value from -0.08 to -0.16 in the nematic

phase, between 32 °C and 27 °C (see Table 1). These order parameters can be factorized as explained in ref. 8 and 22:

$$S_{CF}^{CF_2} = (S_{CF}^{CF_2})^{\text{loc}} S_{\text{agg}} S_{\text{dir}} \quad (8)$$

$(S_{CF}^{CF_2})^{\text{loc}}$ is the order parameter relative to the local director inside the micelle, presumably only weakly dependent on the temperature and sample composition; S_{agg} summarizes the effects of the surface curvature of the aggregates; S_{dir} is the “nematic” order parameter of the aggregates, increasing from ~ 0.2 at the isotropic–nematic transition to ~ 0.7 at the nematic–lamellar one.²³ Interpolated values of $S_{\text{dir}}(T)$ and values of the $(S_{CF}^{CF_2})^{\text{loc}} S_{\text{agg}}$ products computed by eqn (8) are shown in Table 1. As far as S_{agg} is concerned, it is determined by the aggregates size and shape, two properties thoroughly investigated in ref. 11 and 23. S_{agg} might range between 0.6 and 0.8, but, in effects, $S_{\text{agg}} \sim 0.7$ is probably appropriate to all the cases here presented. The estimated values of $(S_{CF})^{\text{loc}}$ are shown in the last column of Table 1. These values agree very well with those reported in the literature for the isotropic²¹ and lamellar phases.²² Moreover, as already found for these two phases, also in the nematic one $(S_{CF}^{CF_2})^{\text{loc}}$ is relatively high and almost uniform along the PFO chain.

Pyridine-d₅ in CsPFO/D₂O

The presence of a considerable amount of pyridine-d₅ alters the phase transition temperatures of the CsPFO/D₂O system, which becomes nematic only below 24.9 °C. The nematic character of the mesophase in the range 24.9 °C–20.1 °C can be inferred observing that the D₂O quadrupolar splitting value and its steep temperature trend closely match those found in the nematic phase of the binary CsPFO/D₂O mixture in the range 32.5 °C–26.5 °C (see Fig. 1).

In the ²H-NMR spectra of pyridine-d₅ in the nematic phase, beside the very strong peaks of D₂O, all the solute signals can be clearly detected (Fig. S3 in ESI†). Each deuterium resonance is split into a doublet by the quadrupolar coupling and all the splittings regularly increase with decreasing temperature. The weakest doublet, with the largest splitting (ranging from 16 kHz to 33 kHz with decreasing temperature), is relative to the para deuterium; the two other doublets (with splittings ranging from 2300 to 4500 Hz and from 600 to 1000 Hz, respectively) are further split into triplets by the dipolar coupling between neighbouring ortho and meta deuterons (the splitting ranges from about 20 to 40 Hz).

In the case of pyridine-d₅ (*C*_{2v} symmetry point group) the molecular frame in which the Saupe matrix is diagonal has one axis, *z*, along the ring para axis and another one, *y*, perpendicular to the molecular plane.¹⁸ By using eqn (4) and (3), each quadrupolar splitting can be expressed as

$$\Delta\nu_q^i = \left| \frac{3}{2} q_{aa}^i \left\{ S_{zz} \left[c_i^2 - \frac{s_i^2}{2} (1 - \eta^i) \right] + \frac{\text{Biax}}{2} \left[s_i^2 + \frac{\eta^i}{3} (1 + c_i^2) \right] \right\} \right| \quad (9)$$

S_{zz} and $S_{xx} - S_{yy} = \text{Biax}$ (biaxiality) are the two non-vanishing independent order parameters, c_i and s_i are $\cos \theta_{az}^i$ and $\sin \theta_{az}^i$, respectively, with the θ_{az}^i angle between the C–D^{*i*} bond direction, *a*, and the *z* axis of the molecule. The

Table 1 Orientational order parameters of the C–F directions of CsPFO in D₂O (see eqn (8)). S_{dir} has been interpolated from ref. 23 and S_{agg} has been assumed to be 0.7. The values of $S^{\text{loc}} \times S_{\text{agg}}$ have been obtained from eqn (8). Estimated uncertainties are ± 0.01

Phase and temperature	$S_{CF}^{CF_2}$ and $S_{CF}^{CF_3}$	S_{dir}	$(S_{CF}^{CF_2})^{\text{loc}} \times S_{\text{agg}}$ and $(S_{CF}^{CF_3})^{\text{loc}} \times S_{\text{agg}}$	$(S_{CF}^{CF_2})^{\text{loc}}$ and $(S_{CF}^{CF_3})^{\text{loc}}$
Isotropic phase, from ref. 21, 22				–0.29 to –0.36 –0.16
Nematic phase, this work				
32 °C	–0.08 –0.03	0.38	–0.21 –0.07	–0.30 –0.11
29 °C	–0.13	0.53	–0.24	–0.34
27 °C	–0.16	0.68	–0.24	–0.34
Lamellar phase, from ref. 22	–0.20 to –0.23 –0.07	0.9	–0.22 to –0.26 –0.08	–0.31 to –0.37 –0.14

expression of the ortho–meta (om) dipolar splitting is obtained from eqn (5) and (6b), considering that the om direction is essentially collinear to the z axis and that the J_{om}^{iso} value is negligible, being less than 0.2 Hz. Therefore:

$$\Delta\nu_{\text{dip}}^{\text{om}} = 2 \cdot \left| -\frac{K_{DD}}{r_{\text{om}}^3} S_{zz} \right| \quad (10)$$

where $K_{DD} = 2830.3 \text{ Å}^3 \text{ s}^{-1}$.

The set of four experimental data, obtained at each temperature, can be fitted to eqn (9) and (10): the fit parameters are S_{zz} and B_{iax} , while the values of q_{aa}^i , η^i , r_{om} and of the relevant angles are assumed from the literature where all these quantities have been accurately estimated using various thermotropic liquid crystalline phases.^{14,16}

In order to perform the fitting, the signs of the splittings must be presumed. The fact that $\Delta\nu_q^{\text{para}}$, which is substantially determined by S_{zz} , is considerably larger than $\Delta\nu_q^{\text{ortho}}$ and $\Delta\nu_q^{\text{meta}}$, reasonably indicates that pyridine roughly behaves like a cylinder with its axis along z , averagely well aligned to the magnetic field. Therefore, the positive sign is assigned to S_{zz} , $\Delta\nu_q^{\text{para}}$ turns out to be positive and $\Delta\nu_{\text{dip}}^{\text{om}}$ negative. Since no indications could be obtained on the signs of $\Delta\nu_q^{\text{ortho}}$ and $\Delta\nu_q^{\text{meta}}$, the data fitting has been tried with various sign combinations and exchanging the assignment of the two small quadrupolar splittings, at each temperature. The results allowed us to unequivocally assign the smallest splitting to the ortho deuterons and to conclude that $\Delta\nu_q^{\text{meta}}$ and $\Delta\nu_q^{\text{ortho}}$ are negative. The compatibility of the data with the known geometry was also confirmed, and, with corrections of just 0.1° to the relevant angles, the fit reproduced all the splittings far within the experimental uncertainty. The obtained S_{zz} values are reported in Fig. 2 *versus* the temperature; the B_{iax} values (not reported) range from 0.003 to 0.007.

Before discussing the results obtained it is useful to consider the chemical species present in solution. The concentration of pyridinium cation, which at the measured pH value of 8.8 can be estimated at about $6 \times 10^{-6} \text{ M}$, corresponds to an amount undetectable in our spectra. Assuming a $\text{pK}_b = 8.75$ for the basic dissociation of pyridine in water, an equilibrium concentration of free pyridine of about 0.02–0.03 M can be estimated. The comparison with the total pyridine concentration ($\sim 0.6 \text{ m}$) indicates that each molecule spends most of its time complexed to micelles. Therefore the order parameters obtained are essentially those of pyridine linked to the micelle. Moreover, considering a CsPFO aggregation number of

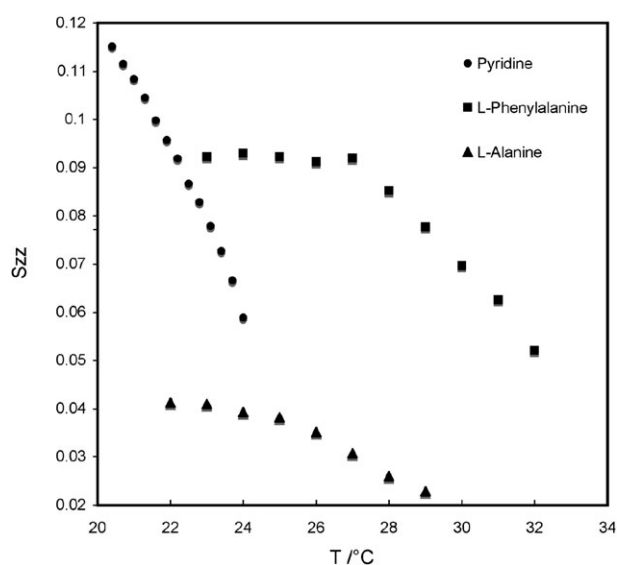


Fig. 2 Trend with temperature of the order parameter S_{zz} of pyridine- d_5 in the nematic phase, and of L-alanine and L-phenylalanine- d_8 in the nematic and lamellar phases of CsPFO/D₂O.

~ 200 – 250 ,¹⁰ the micellar concentration should be $\sim 0.05 \text{ m}$: this means that about 10 pyridine molecules surround each micelle, substantially altering the composition of its first solvation sphere, which can explain the observed noticeable lowering of the isotropic–nematic transition temperature (see Fig. 1).

As far as the molecular average orientation is concerned, the quite high values of S_{zz} (see Fig. 2) and the small values of biaxiality point to an almost cylindrical orientational behaviour of pyridine, which strictly resembles that of the pyridine- I_2 and $-\text{Br}_2$ complexes in the nematic solvents described in ref. 14 and 24, respectively. A sensible picture of the micelle–pyridine interaction is suggested: while the disk-like aggregate orients with its flatter surfaces mainly perpendicular to the magnetic field, pyridine arranges with its para axis mainly perpendicular to the aggregate surface. A specific interaction between the pyridine N atom and a carboxylate group on the micelle surface can easily occur through an intermediate water molecule: in the recent literature, the pyridine–water hydrogen bonding²⁵ and the water–carboxylate groups interaction on the CsPFO micelles surface²⁶ have been studied and described in detail.

L-Alanine and L-alanine- ^{15}N in CsPFO/D $_2\text{O}$

The following analysis takes advantage of the comparison between spectra recorded on L-alanine and L-alanine- ^{15}N . We focus on the ^1H -NMR and ^{13}C -NMR spectra obtained in the isotropic phase of CsPFO/D $_2\text{O}$, in the nematic one at 28 °C and in the lamellar one at 24 °C. The atom labelling used is shown in Fig. 3. The ^1H -NMR spectra in the isotropic phase showed well-resolved H^α - H^{Met} and H^{Met} - ^{15}N scalar couplings, while a maximum value for the H^α - ^{15}N coupling could be estimated from the H^α signals linewidth. From the isotropic ^{13}C -NMR spectra the C^α - H^α , C^α - ^{15}N and C^{Met} - H^{Met} scalar couplings were determined. All these J^{iso} values are collected in Table 2 (for the J signs see ref. 27), together with the relevant dipolar splittings discussed in the following.

In the nematic and lamellar phases the structure of the proton spectra is substantially determined by the ^1H - ^1H dipolar couplings (Fig. 3a), which however are small enough to give rise to first order spectral patterns. In the ^{13}C -NMR spectra of L-alanine (Fig. 3b), the C^α signal is a doublet, because of the scalar and dipolar couplings with H^α . A much smaller splitting is also measurable in the ^{13}C -NMR spectra of L-alanine- ^{15}N , due to the C^α - ^{15}N coupling. The C^{Met} resonance (Fig. 3b) consists of a group of signals which can be interpreted as a quartet, due to the C^{Met} - H^{Met} coupling, split by the interaction with H^α .

In order to determine a unique set of D_{ij} couplings values from the described splittings by eqn (6a) and (6b), at least some D_{ij} 's signs should be inferred. Looking at the data of Table 2 and at eqn (6b), since relatively large $|D_{ij}|$ values are expected to increase with decreasing temperature, we see that

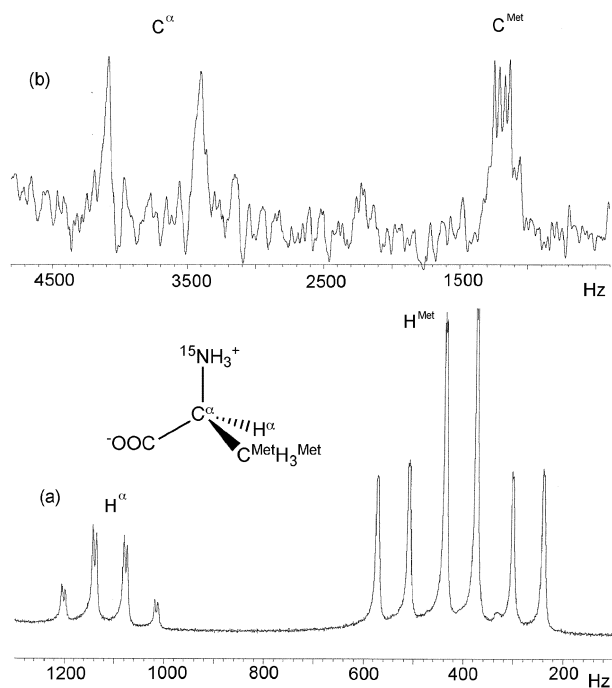


Fig. 3 (a) ^1H spectrum of L-alanine- ^{15}N and (b) ^{13}C spectrum of L-alanine, in the nematic phase of CsPFO/D $_2\text{O}$ ($T = 28$ °C). In the inset the molecular structure of L-alanine- ^{15}N with the atom labeling used in the text is shown.

the C^{Met} - H^{Met} splitting must be positive, and the corresponding dipolar coupling negative. Moreover, if eqn (7) is at least approximately valid, the C^{Met} - H^{Met} and the H^{Met} - H^{Met} dipolar couplings have the same (negative) sign, while the H^α - H^{Met} couplings are likely positive. As far as the signs of the C^{Met} - H^α and C^α - H^α splittings are concerned, they were decided by the results of the data analysis described below, attempted with various signs combinations. The signs of the three small last splittings were also decided by the results of the fitting of the various possible sets of dipolar couplings.

It is well known that alanine essentially exists as a zwitterion at $\text{pH} \sim 7.8$,²⁸ as measured in our lyotropic solutions. Therefore, the minimum energy conformation of L-alanine in its zwitterionic form, reported in ref. 17, was assumed for the dipolar couplings analysis. The molecular reference frame (x, y, z) was chosen with the z axis along the $\text{N}-\text{C}^\alpha$ bond and the x one in the plane defined by the $\text{N}-\text{C}^\alpha$ and $\text{C}^\alpha-\text{H}^\alpha$ bonds. Using eqn (5) and (3), each dipolar coupling was expressed as a linear combination of 5 independent Saupe matrix elements. By fitting the experimental data, at both 28 °C and 24 °C, a set of dipolar couplings was singled out at each temperature (Table 2), excellently consistent with the assumed molecular structure and with physically acceptable order parameters (all the fit residuals were within the experimental error) (reported in Table S1 in the ESI†).

By diagonalizing the Saupe matrix, the principal axes frame (x^D, y^D, z^D) of the order tensor was localized on the molecule (see Fig. 4) and the corresponding order parameters were obtained. At 28 °C and 24 °C the S values were: $S_{xx}^D - 0.015$ and -0.024 , $S_{yy}^D - 0.010$ and -0.015 , $S_{zz}^D 0.026$ and 0.039 . The location of the principal order frame is, as due, essentially the same at 28 °C and 24 °C. Using such a frame, any dipolar coupling is given by a linear combination of only two independent order parameters, S_{zz}^D and $S_{xx}^D - S_{yy}^D = \text{Biax}^D$ (biaxiality). Therefore, the orientational analysis could be extended to the whole temperature range from 29 °C to 22 °C, where ^1H anisotropic spectra had been recorded: the S_{zz}^D values, computed at each temperature from the H^α - H^{Met} and H^{Met} - H^{Met} dipolar couplings, are shown in Fig. 2. The Biax^D values (not reported) ranged between -0.004 and -0.005 .

The best aligned molecular axis, z^D , forms angles of $\sim 63^\circ$, $\sim 62^\circ$, $\sim 85^\circ$ and $\sim 152^\circ$ with the $\text{C}^\alpha-\text{N}$, $\text{C}^\alpha-\text{C}^{\text{Met}}$, $\text{C}^\alpha-\text{H}^\alpha$ and $\text{C}^\alpha-\text{COO}^-$ bond directions, respectively. The S_{zz}^D values are positive, while S_{xx}^D and S_{yy}^D are negative and give relatively low order biaxiality: therefore, the average orientational behaviour of alanine is roughly cylindrical around the z^D axis. All this suggests that the crucial character of the alanine-micelle interactions is the removal of the carboxylic group from the proximity of the micelle surface. In effect, the NH_3^+ group certainly forms relatively stable hydrogen bonds with the carboxylic groups on the micelle surface, as confirmed by the fact that ammonium is a good counterion for the formation of PFO $^-$ micelles giving a nematic phase¹²; moreover, a recent Molecular Dynamics study of the interaction between alanyl-phenylalanyl-alanine and CsPFO micelles²⁹ shows that the mean times spent by the NH_3^+ and COO^- groups far (3.5 Å apart) from one or more PFO molecules are 79 ps and 2395 ps, respectively, with a ratio of 1:30.

Nuclear pair	J^{iso}/Hz	$\Delta\nu$ (28 °C)/Hz	$\Delta\nu$ (24 °C)/Hz	D (28 °C)/Hz	D (24 °C)/Hz
$\text{H}^\alpha\text{--H}^{\text{Met}}$	7.3	62	80.3	27	37
$\text{H}^\alpha\text{--}^{15}\text{N}$	≈ 1.8	6.9	6.1	−5	−4
$\text{H}^{\text{Met}}\text{--H}^{\text{Met}}$	0	134.4	185.4	−45	−62
$\text{H}^{\text{Met}}\text{--}^{15}\text{N}$	2.6	3.6	2.9	−3.1	−2.8
$\text{C}^\alpha\text{--H}^\alpha$	144	724	896	290	376
$\text{C}^\alpha\text{--}^{15}\text{N}$	−4.6	9.2	18	−3	−7
$\text{C}^{\text{Met}}\text{--H}^\alpha$	−4.4	38.7	49.6	22	27
$\text{C}^{\text{Met}}\text{--H}^{\text{Met}}$	129.9	84.4	49.6	−23	−40

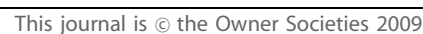


Table 3 Experimental deuterium quadrupolar splittings ($\Delta\nu_q$) and dipolar coupling constants (D) of L-phenylalanine- d_8 and L-phenylalanine, determined in the lamellar phase of CsPFO/water at 25 °C. Experimental uncertainties are about 200 Hz on quadrupolar splittings, 2–5 Hz or 5–10 Hz on dipolar couplings not involving or involving H^z , respectively

Nucleus	$\Delta\nu_q$ (Hz)
D^{para}	16 500
D^{meta}	–6150
D^{ortho}	–5900
$D^{Me(I)}$	–13 000
$D^{Me(II)}$	–9850
$ D^z $	15 250
Nuclear pair	D (Hz)
$D^{meta}-D^{ortho}$	–42
$D^{Me(I)}-D^{Me(II)}$	82
$H^{ortho}-H^{meta}$	–452
$H^{ortho}-H^{para}$	–48
$H^{ortho}-H^{meta/}$	22
$H^{ortho}-H^{ortho/}$	75
$H^{meta}-H^{para}$	175
$H^{meta}-H^{meta/}$	74
$H^{Me(I)}-H^{Me(II)}$	871
$H^{Me(I)}-H^{ortho}$	–25
$H^{Me(I)}-H^{meta}$	–20
$H^{Me(I)}-H^{para}$	–25
$H^{Me(II)}-H^{ortho}$	–10
$H^{Me(II)}-H^{meta}$	–35
$H^{Me(II)}-H^{para}$	–35
H^z-H^{ortho}	–40
H^z-H^{meta}	–30
H^z-H^{para}	–30
$ (H^z-H^{Me(I)}) + (H^z-H^{Me(II)}) $	60

As far as the methylenic fragment is concerned, we assumed a regular tetrahedral geometry for the bonds involving the C atom, with a CD bond length of 1.12 Å. From the $D^{Me}-D^{Me}$ dipolar coupling the order parameter of the internuclear direction, S_{DD}^{Me} , was obtained by eqn (5); its absolute value was 0.044. Whichever the conformation around the $C^{Me}-C^{Phen}$ bond, the $D^{Me}-D^{Me}$ internuclear direction is perpendicular to the z (or para) direction of the aromatic ring. We had already determined $S_{xx} = -0.050$ and $S_{yy} = -0.010$: comparing these values with the absolute value of S_{DD}^{Me} , we could assign a negative sign to S_{DD}^{Me} and infer that the $D^{Me}-D^{Me}$ average direction is approximately collinear with the ring x axis. Using eqn (3) and (4) and roughly supposing that the $D^{Me}-D^{Me}$ and z directions were principal axes of the order tensor of the methylenic fragment, we could also estimate the order parameters for the two $C-D^{Me}$ directions: since these form equal angles with the assumed principal axes, two equal order parameters $S_{CD}^{Me} = -0.028$ were obtained. Actually, the two experimental splittings are different and the experimental absolute values of the S_{CD}^{Me} order parameters, determined by means of eqn (5), are 0.035 and 0.040. Even if all this clearly indicates that our assumption about the order principal axes frame is not satisfying, nevertheless at least the negative sign of S_{CD}^{Me} is presumably reliable. Therefore, we give a negative sign to the quadrupolar splittings of both methylenic deuterons.

Finally, the D^z quadrupolar splitting is considered. Its absolute value is very similar to that of the aromatic para deuteron splitting. If the two splittings have the same sign, the

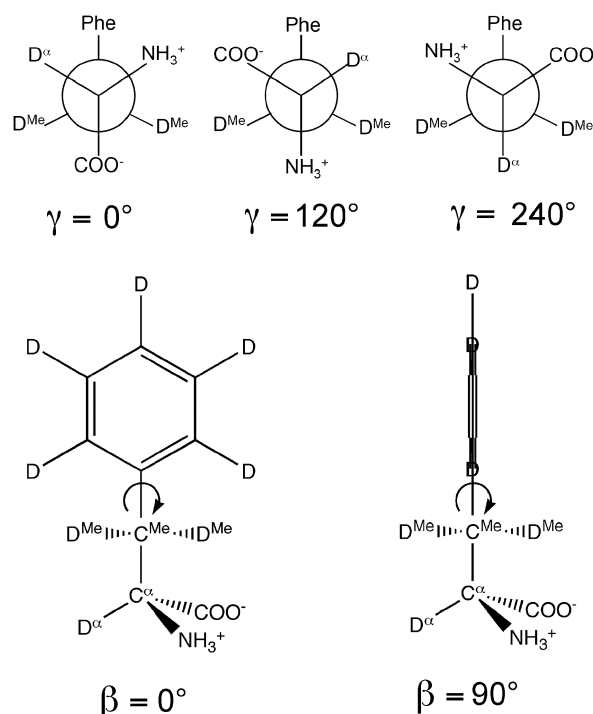


Fig. 6 Sketches of the molecular conformations of L-phenylalanine- d_8 corresponding to the reported values of γ and β angles.

$C-D^{para}$ and $C-D^z$ directions could be more or less parallel, and the staggered molecular conformation corresponding to $\gamma = 240^\circ$ shown in Fig. 6 should be prevailing. On the other hand, if the two splittings have different signs, the two conformations with $\gamma = 0^\circ$ or $\gamma = 120^\circ$ could be preferred.

The 1H spectrum of L-phenylalanine in CsPFO/ D_2O at 25 °C is shown in Fig. 7a. Its complex structure is due to the

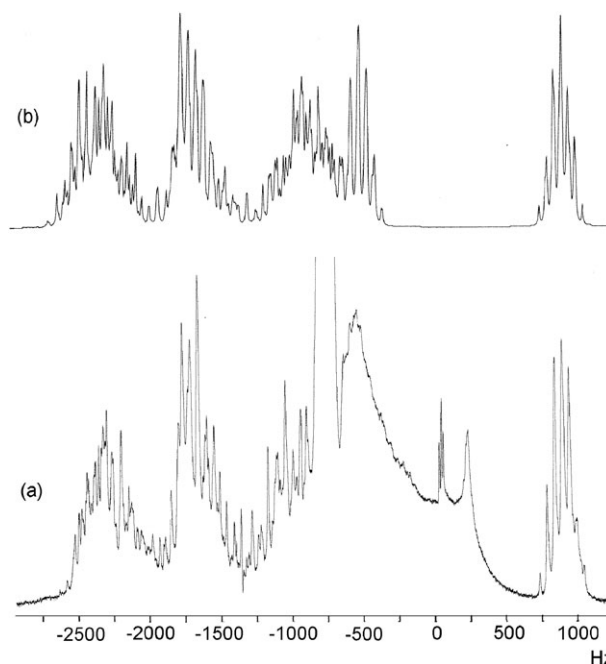


Fig. 7 (a) 1H experimental and (b) simulated spectra of L-phenylalanine in the lamellar phase of CsPFO/ D_2O ($T = 25^\circ C$).

high number of homonuclear dipolar interactions. The proton dipolar couplings were determined by simulating the spectrum (by the LEQUOR program³⁰) until the best fit one was obtained by visual inspection. As a first step, the values of the aromatic H–H dipolar couplings and of the intra-methylene one were computed, by means of eqn (5) and (3), from the local order parameters obtained from the deuterium data. Then, trial inter-fragment dipolar couplings, also involving H^α, were gradually included. The best simulated rather satisfactory spectrum is shown in Fig. 7b and the corresponding dipolar couplings are reported in Table 3. The signs and values of the dipolar couplings between methylenic and aromatic protons are well determined, while the dipolar couplings involving H^α are affected by higher uncertainties, due to the fact that important signals were hidden by the HDO intense peak. As far as the couplings between H^α and the two methylenic protons are concerned, their sum was found to influence the spectrum rather than their individual values. Therefore this sum will be considered the reliable experimental datum.

Global analysis of data from ¹H and ²H NMR spectra and discussion

In the following analysis two torsion angles were considered, β and γ , describing the rotations around the C^{Me}–C^{Phen} and C^α–C^{Me} bonds, respectively. The conformational condition corresponding to $\beta = \gamma = 0$ is sketched in Fig. 6.

As far as the determination of β is concerned, the fitting of the data set involving the phenyl and methylenic groups was attempted using a single conformer model, that is considering the rotation of the phenyl ring around its para axis, restricted to a 180° flip motion between two identical minimum energy conformations, characterized by a value of β . We assumed standard values for bond lengths and angles and fixed a molecular frame with the z axis along the C^α–C^{Me} bond and the x axis along the H^{Me}–H^{Me} internuclear direction, as shown in Fig. 5. The experimental quadrupolar and dipolar couplings at 25 °C were contemporarily fitted to eqn (4) and (5), combined with eqn (3), respectively. The fitting parameters were the five order parameters of the considered molecular fragment and the β angle. The fitting procedure terminated with a good reproduction of all the experimental data, provided that the tetrahedral structure of the methylenic carbon was altered by decreasing the angle between the C^{Me}–C^{Phen} and C^α–C^{Me} bonds to 105°. β was found to be 10°, confirming that, as already inferred from the deuterium data only, the H^{Me}–H^{Me} direction is approximately collinear with the ring x axis. By diagonalizing the Saupe matrix, the order parameters relative to the principal axes frame sketched in Fig. 8 were obtained. The principal order parameter S_{zz}^D is relatively high (0.093), while the order biaxiality $S_{xx}^D - S_{yy}^D$ is low (–0.017). More refined models have been attempted to fit the experimental data, including trial distributions of β , but all these trials brought back one conformer model, which was finally accepted as the best one.

For studying the conformation around the C^α–C^{Me} bond, described by the γ angle, the couplings involving H^α and D^α

were added to the data set. In order to test the compatibility of the simple one-conformer hypothesis with the experimental data reported in Table 3, their global fitting was performed, determining the five order parameters and γ . The β and C^{Phen}–C^{Me}–C^α angles were fixed as previously determined, while standard values of C^α–C^{Me} (1.53 Å), C^α–H^α (1.12 Å) and of the angle C^{Me}–C^α–H^α (109.5°) were assumed. The four possible combinations of the two unknown signs (relative to the D^α quadrupolar splitting and to the sum of the two H^α–H^{Me} dipolar couplings) were attempted, but in no case was the single conformer model able to satisfactorily reproduce all the experimental data within their experimental error. Indeed, this fact indicates that the conformational and orientational models describing the whole molecule should be more refined, including vibrational corrections and a distribution of γ values around the minimum energy conformations, and also allowing the order parameters to vary with the conformation itself.³¹ Nevertheless, some useful considerations are possible on the basis of the single conformer fitting results, if we presume that the Saupe matrix determined for the phenyl–methylene fragment fairly describes the average order of the whole molecule in its most populated conformation. In fact, the fitting quality, even if poor, was at its best around the staggered conformation with $\gamma = 120^\circ$, a condition where the best fit order parameters and the location of the principal order frame were in substantial agreement with those determined for the phenyl–methylene fragment. Therefore, a conformer with $\gamma \simeq 120^\circ$ is suggested to be prevailing or, at least, to be an “effective” one.

It is worth looking at the location of the principal order frame in this conformer, keeping in mind that phenylalanine essentially exists as a zwitterion at pH ~ 7.8 .²⁸ As shown in Fig. 8, the NH₃⁺ group and the aromatic ring are as far as possible from each other and the best-ordered molecular axis, z^D , is almost parallel to both directions connecting the aromatic ring to H^α and to the NH₃⁺ group, forming angles of 9° and 12°, respectively. A simple interpretation of this arrangement is straightforward: the zwitterionic head of the molecule, in particular the NH₃⁺ group, approaches the discotic micelle surface, while the aromatic ring points far from it. The reliability of this conclusion is supported by the previously cited Molecular Dynamics study²⁹ on the interaction between alanyl–phenylalanyl–alanine and CsPFO micelles. Moreover, the conformer of phenylalanine with $\gamma \sim 120^\circ$ was found to be the most stable in polar solvents, in particular in water, by the analysis of the isotropic J couplings.³² Various recent computational and experimental determinations of stable conformations of L-phenylalanine are present in the literature, but the cases investigated cannot be considered good models of zwitterionic L-phenylalanine in a complex and interacting solvent.^{33–35}

Finally, assuming the conformer with $\beta = 10^\circ$ and $\gamma = 120^\circ$ as the “effective” one, it was easy to obtain, through eqn (4) and (3), five molecular order parameters from the five quadrupolar splittings observed in the ²H-NMR spectra of L-phenylalanine-d₈, recorded in the temperature range from 33 °C to 23 °C. By means of a fitting procedure, a single rotation matrix excellently diagonalizing all the Saupe matrices relative to the various temperatures was found. The

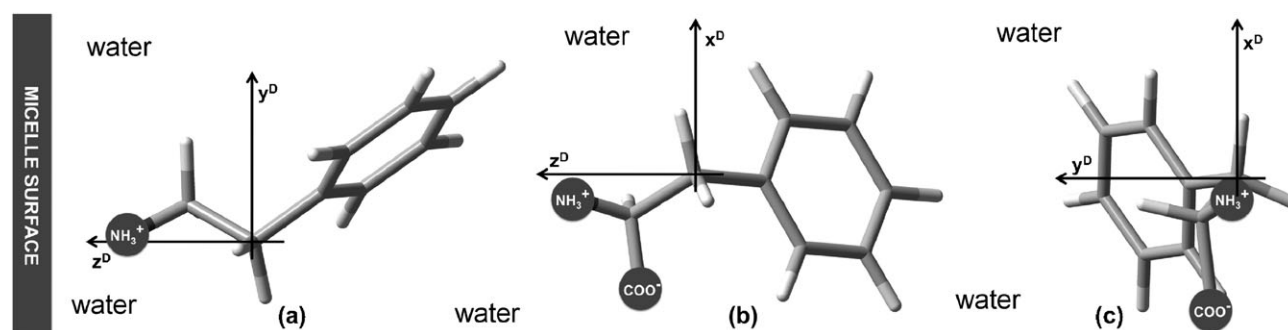


Fig. 8 Location of the principal axis frame in the conformer of L-phenylalanine with $\gamma \sim 120^\circ$ and its preferred orientation with respect to the micelle surface, as seen along the (a) x^D , (b) y^D , (c) z^D axes.

temperature trend of the principal order parameter, S_{zz}^D , ranging between 0.052 and 0.093, is shown in Fig. 2, while the order biaxiality $S_{xx}^D - S_{yy}^D$ varies between -0.012 and -0.020 . Finally, we verified that the S_{zz}^D values are only weakly dependent ($\pm 10\%$) on relatively small changes of γ ($\mp 15^\circ$), while the biaxiality is more sensitive, for instance it is reduced to about $-0.002/-0.003$ for $\gamma = 105^\circ$.

Conclusion

The local orientational order parameters of the PFO chain inside the micelles, here determined in the nematic phase of CsPFO/water, turned out to be very similar to those already reported in the literature for both the isotropic and lamellar phases.^{21,22}

By exploiting the traditional multinuclear LX-NMR approach, orientational and structural/conformational parameters of pyridine, L-alanine and L-phenylalanine dissolved in the nematic and lamellar phases of CsPFO/water have been obtained. The order parameters S_{zz} of the three solutes here studied reach values similar to or slightly lower than those measured on the same or similar molecules in thermotropic liquid crystalline phases.^{14,24,36,37} This indicates that, in all the three cases, a relevant fraction of solute interacts with the ordered micelles and that such an interaction is rather specific, even in the case of a small, almost globular molecule like L-alanine. The interpretation of the orientational behaviour of the pyridine-micelle “complex” is quite straightforward, while in the more complex cases of L-alanine and, in particular, of the flexible L-phenylalanine, our orientational and conformational findings are supported by—and support—the results of a recent Molecular Dynamics study.²⁹ Reasonable pictures of the relative solute-micelle arrangements have been proposed in all the cases. In particular, for the flexible L-phenylalanine, whose interaction with the micelle might affect the conformational distribution, an “effective” conformer has been obtained by the NMR data, whose orientational behaviour suggests a physically convincing interaction with the micelle surface.

Acknowledgements

The authors are grateful to Dr Alberto Marini for helpful discussions.

References

- 1 *Nuclear Magnetic Resonance of Liquid Crystals*, ed. J. W. Emsley, NATO ASI Series, Series C: Mathematical and Physical Sciences, vol. 141, D. Reidel Publishing Company, Dordrecht/Boston/Lancaster, 1983.
- 2 J. W. Emsley and J. C. Lindon, *NMR Spectroscopy Using Liquid Crystal Solvent*, Pergamon Press, Oxford, 1975.
- 3 N. Tjandra and A. Bax, *Science*, 1997, **278**, 1111–1114.
- 4 A. Bax, *Protein Sci.*, 2003, **12**, 1–16.
- 5 C. Landersj, J. L. M. Jansson, A. Maliniak and G. Widmalm, *J. Phys. Chem. B*, 2005, **109**, 17320–17326.
- 6 S. Pizzanelli, S. Monti and C. Forte, *J. Phys. Chem. B*, 2005, **109**, 21102–21109.
- 7 C. F. Weise and J. C. Weissar, *J. Phys. Chem. B*, 2003, **107**, 3265–3277.
- 8 N. Boden, S. A. Corne and K. W. Jolley, *J. Phys. Chem.*, 1987, **91**, 4092–4105.
- 9 N. Boden, K. W. Jolley and M. H. Smith, *J. Phys. Chem.*, 1993, **97**, 7678–7690.
- 10 M. C. Holmes, D. J. Reynolds and N. Boden, *J. Phys. Chem.*, 1987, **91**, 5257–5262.
- 11 N. Boden, S. A. Corne, M. C. Holmes, P. H. Jackson, D. Parker and K. W. Jolley, *J. Physique*, 1986, **47**, 2135–2144.
- 12 N. Boden, J. Clements, K. W. Jolley, D. Parker and M. H. Smith, *J. Chem. Phys.*, 1990, **93**, 9096–9105.
- 13 B. Binks, P. Fletcher, S. Kotsev and R. Thompson, *Langmuir*, 1997, **13**, 6669–6682.
- 14 D. Catalano, C. A. Veracini, P. L. Barili and M. Longeri, *J. Chem. Soc., Perkin Trans. II*, 1983, 171–174.
- 15 D. Catalano, C. Forte, C. A. Veracini and C. Zannoni, *Israel J. Chem.*, 1983, **23**, 283–289.
- 16 R. Ambrosetti, D. Catalano, C. Forte and C. A. Veracini, *Z. Naturforsch.*, 1986, **41a**, 431–435.
- 17 L. Gontrani, B. Mennucci and J. Tomasi, *J. Mol. Struct.-Theochem.*, 2000, **500**, 113–127.
- 18 C. Zannoni, in *Nuclear Magnetic Resonance of Liquid Crystals*, ed. J. W. Emsley, NATO ASI Series, Series C: Mathematical and Physical Sciences, vol. 141, D. Reidel Publishing Company, Dordrecht/Boston/Lancaster, 1983, pp. 1–34.
- 19 J. W. Buchanan, E. Munteanu, B. A. Dawson and D. Hodgson, *Magn. Reson. Chem.*, 2005, **43**, 528–534.
- 20 J. Vaara, J. Kaski and J. Jokisaari, *J. Phys. Chem. A*, 1999, **103**, 5675–5684.
- 21 I. Furó and R. Sitnikov, *Langmuir*, 1999, **15**, 2669–2673.
- 22 S. V. Dvinskikh and I. Furó, *Langmuir*, 2000, **16**, 2962–2967.
- 23 H. Jóhannesson, I. Furó and B. Halle, *Phys. Rev. E.*, 1996, **53**, 4904–4917.
- 24 C. A. Veracini and M. Longeri, *Chem. Phys. Lett.*, 1973, **19**, 592.
- 25 I. Pápai and G. Jancsó, *J. Phys. Chem. A*, 2000, **104**, 2132–2137.
- 26 S. Balasubramanian, S. Pal and B. Bagchi, *Curr. Sci.*, 2003, **84**, 428–430.
- 27 J. B. Stothers, *Carbon-13 NMR Spectroscopy*, Organic Chemistry, Academic Press, New York, 1972, vol. 24.
- 28 D. Voet and J. G. Voet, *Biochemistry*, John Wiley & Sons, 2nd edn, 1995.

- 29 S. Pizzanelli, C. Forte, S. Monti and R. Schweitzer-Stenner, *J. Phys. Chem. B.*, 2008, **112**, 1251–1261.
- 30 P. Diehl, H. P. Kellerhals and W. Niederberger, *J. Magn. Reson.*, 1971, **4**, 352–357.
- 31 In principle, the problem could be tackled by the ME (Maximum Entropy) or AP (Additive Potential) approaches. Anyway, ME requires highly ordered molecules, while AP requires the knowledge of suitable interaction coefficients. A new promising approach, recommended for the analysis of residual couplings in flexible molecules, is the combined APME method applied until today to a limited number of rich data sets, see for instance: C. Landersjö, B. Stevansson, R. Eklund, J. Östervall, P. Söderman, G. Widmalm and A. Maliniak, *J. Biomol. NMR*, 2006, **35**, 89–101.
- 32 R. A. Newman and M. A. Miller, *J. Phys. Chem.*, 1971, **75**, 505–508.
- 33 J. P. Simons, *C. R. Chimie*, 2003, **6**, 17–31.
- 34 T. Ebata, T. Hashimoto, T. Ito, Y. Inokuchi, F. Altunsi, B. Brutschi and P. Tarakeshwar, *Phys. Chem. Chem. Phys.*, 2006, **8**, 4783–4791.
- 35 G. von Helden, I. Compagnon, N. M. Blom, M. Frankowski, U. Erlekam, J. Oomens, B. Brauer, R. B. Gerber and G. Meijer, *Phys. Chem. Chem. Phys.*, 2008, **10**, 1248–1256.
- 36 E. E. Burnell, C. A. de Lange, J. B. S. Barnhoorn, I. Aben and P. F. Levelt, *J. Phys. Chem. A*, 2005, **109**, 11027–11036.
- 37 D. Catalano, G. Celebre, J. W. Emsley, M. Longeri, G. De Luca and C. A. Veracini, *J. Chem. Soc., Perkin Trans. 2*, 1998, 1823–1826.